Photosynth Res (2008) 98:179–187
DOI 10.1007/s11120-008-9339-5

REGULAR PAPER

Room temperature photooxidation of β-carotene and peripheral chlorophyll in photosystem II reaction centre

Radek Litvin · David Bina · Frantisek Vacha

Received: 25 April 2008 / Accepted: 23 July 2008 / Published online: 4 September 2008

Abstract Differential kinetic absorption spectra were measured during actinic illumination of photosystem II reaction centres and core complexes in the presence of electron acceptors silicomolybdate and ferricyanide. The spectra of samples with ferricyanide differ from those with both ferricyanide and silicomolybdate. Near-infrared spectra show temporary β-carotene and peripheral chlorophyll oxidation during room temperature actinic illumination. Peripheral chlorophyll is photooxidized even after decay of β-carotene oxidation activity and significant reduction of β-carotene content in both reaction centres and photosystem II core complexes. Besides, new carotenoid cation is observed after about 1 s of actinic illumination in the reaction centres when silicomolybdate is present. Similar result was observed in PSII core complexes. HPLC analyses of illuminated reaction centres reveal several novel carotenoids, whereas no new carotenoid species were observed in HPLC of illuminated core complexes. Our data support the proposal that pigments of inner antenna are a sink of cations originating in the photosystem II reaction centre.

Keywords Photosystem II · Reaction centre · β-Carotene · Oxidation · Silicomolybdate · Ferricyanide

R. Litvin · D. Bina · F. Vacha (✉)
Biology Centre of AVCR, v.v.i., Institute of Plant Molecular Biology, Branisovska 31, 370 05 Ceske Budejovice, Czech Republic
e-mail: vacha@jcu.cz

R. Litvin · D. Bina · F. Vacha
Faculty of Science, University of South Bohemia, Branisovska 31, 370 05 Ceske Budejovice, Czech Republic

F. Vacha
Institute of Physical Biology, University of South Bohemia, Zamek 136, 373 33 Nove Hrady, Czech Republic

Abbreviations

β-Car	β-Carotene
5ChlRC	Five-chlorophyll isolation of PSII RC
Car	Carotenoid
CarD1, CarD2	β-Carotene in D1, D2 protein, respectively
Chl	Chlorophyll
ChlD1, ChlD2	Accessory chlorophylls of PSII RC located in D1, D2, respectively
Chl_Z^+	Cation of one (or both) peripheral chlorophyll(s)
Chl_ZD1, Chl_ZD2	Peripheral chlorophyll of D1, D2 proteins, respectively
Cyt b_{559}	Cytochrome b_{559} of PSII RC
DM	*n*-Dodecyl-β-D-maltoside
EPR	Electron paramagnetic resonance
FeCy	Potassium ferricyanide
HPLC	High performance liquid chromatography
MES	2-(*N*-Morpholino)ethanesulphonic acid
NIR	Near-infrared electromagnetic region
P680	Primary donor of PSII
PSII	Photosystem II
PSII core	Complex of PSII RC and inner antennae CP43 and CP47
PSII RC	Photosystem II reaction centre (D1/D2/Cyt b559/PsbI complex)
SiMo	Silicomolybdate

Introduction

Photosystem II (PSII) is a membrane-bound enzymatic pigment–protein complex which catalyses electron transfer from water to plastoquinone. The core of PSII is composed of a reaction centre (PSII RC) and inner antennae CP43 and

CP47. The isolated PSII RC consists of D1/D2, Cyt b_{559} and PsbI proteins and contains six chlorophyll *a* and two pheophytin *a* molecules, one or two β-carotenes and one heme of the cytochrome. Inner antennae contain 29 chlorophylls *a* and 9 β-carotenes (Loll et al. 2005).

Four of the six chlorophylls of PSII RC located near the centre and close to each other are probably excitonically coupled and form primary electron donor P680 (Durrant et al. 1995; Raszewski et al. 2008). Two of them are analogical to the special pair of purple bacteria reaction centres. The other two are called accessory chlorophylls and sometimes denoted ChlD1 and ChlD2, based on their location. The remaining two Chls are called peripheral chlorophylls and do not have an analogy in the purple bacteria reaction centre. They are often denoted as Chl_ZD1 and Chl_ZD2 and are symmetrically located on the opposite sides of the PSII RC. The Chl_ZD2 is on the same side of the PSII RC as the Cyt b_{559}; however, the centre to centre distance between the Cyt b_{559} heme and the Chl_ZD2 ring is about the same as between the Chl_ZD2 and ChlD2 of P680 (26.3 vs. 24.3 Å, respectively, Loll et al. 2005).

The two β-carotenes of PSII RC are located in D1 and D2. Their absorption maxima are presumed to be 489 nm (CarD1) and 507 nm (CarD2) based on agreement of their respective LD spectra and their positions within the PSII RC (Tomo et al. 1997; Ishikita et al. 2007). The CarD1 is located between the Chl_ZD1 and P680, very close to the Chl_ZD1 (at a distance of 4.1 Å). The CarD2 is located in between the Cyt b559 heme, Chl_ZD2 and ChlD2 of P680. The CarD1 has several β-carotene molecules of CP47 inner antenna in proximity as opposed to the CarD2 which is more distant from other carotenes (Ishikita et al. 2007).

Besides the main electron pathway in PSII which consists of manganese cluster of oxygen evolving complex, one redox active tyrosine TyrZ (tyrosine 161 of D1 protein) residue, primary donor (P680), D1-pheophytin *a* and two plastoquinones, alternative electron pathways were proposed to be functional under certain circumstances. Oxidized primary donor ($P680^+$) is the most positive charge found in a living matter, and if not reduced by an electron originating from the water it can extract electrons from its neighbourhood. In the case of unspecific oxidation of the PSII RC protein matrix, a permanent damage can be done resulting in inhibition of PSII function. It has been proposed that the cofactors preferentially oxidized by long-lived $P680^+$ are the β-carotene(s) of PSII RC, one or both peripheral chlorophyll(s) and the heme of Cyt b_{559} (see e.g. Frank and Brudvig 2004).

Several photooxidation pathways have been proposed. Ishikita et al. (2007) recently suggested the CarD2 to be the primary electron donor to $P680^+$ subsequently reduced by either Cyt b_{559} heme or Chl_ZD2 with the heme being the faster donor. However, earlier studies suggested that both peripheral chlorophylls and both β-Cars can be oxidized. The peripheral chlorophyll *a* cation Chl_Z^+ was assigned to Chl_ZD1 by observing the distortion of resonance Raman spectra by site-directed mutations in *Synechocystis* 6803 PSII core complexes (Stewart et al. 1998). Another group located Chl_Z^+ to D2 by studying the effect of site-directed mutagenesis in *Chlamydomonas reinhardtii* on fluorescence quenching and EPR signal of PSII membranes and PSII RCs (Wang et al. 2002). Tracewell et al. (2001) studied NIR, Raman and EPR spectra of *Synechocystis* and spinach PSII particles and concluded that compared to *Synechocystis* PSII particles where only one Chl_ZD1 was oxidized, in spinach PSII membranes both peripheral chlorophylls were oxidized. Tracewell and Brudvig (2003) observed two distinct β-Car cations with different kinetic behaviour in PSII core complexes of *Synechocystis* and *Synechococcus* and in spinach PSII membranes.

Compared to most of the previous results, we have, in this work, performed a series of room temperature experiments to investigate the alternative electron donor pathways on PSII five-chlorophyll reaction centres and PSII core complexes. We have observed that alternative electron donors operate also at room temperature and, therefore, may have a physiological role in protection of PSII reaction centres from photooxidative damage caused by accumulated $P680^+$ in the case of donor side photoinhibition.

Materials and methods

PSII core complexes were isolated from peas as described in Kuta Smatanova et al. (2006); PSII five-chlorophyll reaction centres (5ChlRC) were prepared from peas according to Vacha et al. (1995) with slight modification described in Vacha et al. (2002). Isolated PSII core and RC complexes were stored at −70°C before use.

Samples were prepared by dilution in an appropriate buffer to a chlorophyll concentration of 40 μg Chl ml^{-1}. The RC buffer contained 50 mM MES pH 6.5 and 0.02% DM; the PSII core buffer contained 50 mM Tris pH 7.2 and 0.02% DM. Electron acceptors were added prior to measurements to a final concentration of 200 μM silicomolybdate (SiMo) and/or 20 mM ferricyanide (FeCy). When needed, oxygen scavenging system of glucose/glucose-oxidase/catalase system (0.3 mg ml^{-1} glucose-oxidase, 70 mM glucose and 0.3 mg ml^{-1} catalase) was used to remove the oxygen from the sample.

Visible–NIR differential optical absorption spectra were measured with a pump-and-probe based instrument described in Bina et al. (2006). Xenon flash lamps are used for both pump and probe; sample and reference rays are dispersed in an imaging monochromator and detected by

two 38 element photodiode arrays. The resolution of the instrument is 2.1 nm in blue region and 6.2 nm in the NIR region. Halogen lamp was used as a source of actinic light giving light intensity of ~1,700 μmol photons m^{-2} s^{-1} inside the cuvette; heat filter in the lamp and either Corning 4-96 for blue light or Coherent RA61 for red light were used. The illumination was controlled by electronic shutter. Sample cell was kept at 0–4°C by a Peltier cooler. Cuvettes with 1 cm optical path length were used for all experiments.

Prior to the measurements of absorbance difference spectra, the sample mixture was left in the spectrometer in the dark for 10 min. First, one dark-adapted spectrum was measured; then the actinic light was turned on, and a series of 47 logarithmically timed measurements were performed during illumination (the first spectrum was taken 18 ms after the actinic light was turned on). After 60 s the actinic light was turned off, and in the 900th second of a dark relaxation two spectra 1 s apart were measured to monitor the relaxation of absorbance transient changes. This illumination experiment was repeated 5–10 times on the same sample.

If needed, absorbance data were processed by in-house written global multiple-gaussian fitting scripts. Global fitting decreases the number of unknown fitted parameters by sharing some of them among multiple spectra. In our case peak positions and widths were set to be identical across the spectra set measured during one experiment. The quality of fits was checked by evaluating residuals, adjusted R^2 and Akaike statistics, fitted parameter's confidence intervals and physical relevance.

Pigment composition was analyzed by HPLC consisting of Pump Controller 600, Delta 600 injection system and a PDA 996 detector (Waters, USA) on a reverse phase ZORBAX ODS column (4.5 × 250 mm, 5 μm, non-end-capped) using an isocratic elution with 100% methanol for 25 min followed by a linear gradient from 100% methanol to a mixture of methanol–hexane (4:1) for 1 min and isocratic elution by the methanol–hexane mixture for another 25 min. The flow rate was 1 ml min^{-1}. For the study of the effect of illumination on the pigment composition, 100 μl of PSII or 5ChlRC sample (at a chlorophyll concentration ~200 μg ml^{-1}) was mixed with 5 μl of 10 mM SiMo and injected into a 1-mm optical path length cuvette. The sample was then illuminated five times for 60 s (at the light intensity of 1,700 μmol photons m^{-2} s^{-1}) with 900 s dark relaxation between the subsequent illuminations. Of the sample, 50 μl were added to 250 μl of 100% acetone and left on ice for 10 min. The mixture was then centrifuged at 7,200*g* for 2 min. Of 100% acetone, 50 μl was added to the pellet, vortexed and immediately centrifuged as above. Supernatants were combined and concentrated under a stream of N_2 gas, then loaded into the HPLC column.

Results

The accumulation of oxidized $P680^+$ and its interaction with the neighbouring pigments was first monitored by the NIR absorption difference spectra in presence of FeCy or a mixture of FeCy and SiMo. The results of these experiments are summarized in Fig. 1. The effect of FeCy electron acceptor on the oxidation of 5ChlRC is in Fig. 1a. In the presence of FeCy, one major absorption change at 730 nm is observed due to P680/$P680^+$ oxidation as was previously observed in Hillmann and Schlodder (1995) and Mathis and Setif (1981). No carotenoid or peripheral chlorophyll cations were observed under these conditions. The small positive peak centred on 965 nm is a water absorption which increases as the sample is slightly heated by prolonged (60 s) actinic illumination. This temperature increase is not compensated for because the reference cell is not illuminated. We have experimentally assigned the size of ~0.0006 A change to the change in temperature of less than 1 K (data not shown).

Huge carotene cation absorption peaking around 950 nm is observed on fresh 5ChlRC samples in the presence of both SiMo and FeCy (Fig. 1b). This absorption transient is quickly depleted by further illumination. No such features were observed on samples that were ever previously illuminated. Another peak at ~820 nm and the absorbance change of $P680^+$ are markedly visible still after 60 s of actinic illumination and are also observed even after 10 subsequent 60 s long illuminations. Based on the amplitude of 680 nm bleaching (not showed) and ~730 nm P680 cation absorption, the $P680^+$ yield is about 10 times higher in the presence of SiMo than if only FeCy is used. We attribute the absorbance change at ~820 nm to the oxidized peripheral chlorophyll Chl_ZD1 in agreement with Tracewell et al. (2001).

PSII core complexes, with FeCy as a single electron acceptor, provide NIR spectra distinctly different from the 5ChlRC (see Fig. 1c). Besides $P680^+$ absorption transition, peripheral chlorophyll cation at 820 nm (Tracewell et al. 2001) and β-carotene cation at 999 nm are observed. The β-Car cation signal at 999 nm is depleted during the prolonged actinic illumination (compare spectra at 1 s and 60 s in Fig. 1c); however, it can still be observed even after several illumination experiments on a single sample (47% of the original signal's amplitude still during the fifth illumination experiment). These results are independent on the presence or absence of oxygen.

Analogically to 5ChlRC, illuminated PSII core complexes exhibit in the presence of a mixture of SiMo and FeCy pronounced NIR absorption changes with large contribution of component(s) between 850 and 950 nm (Fig. 1d). The $P680^+$ yield is also about four times higher than if only FeCy is present.

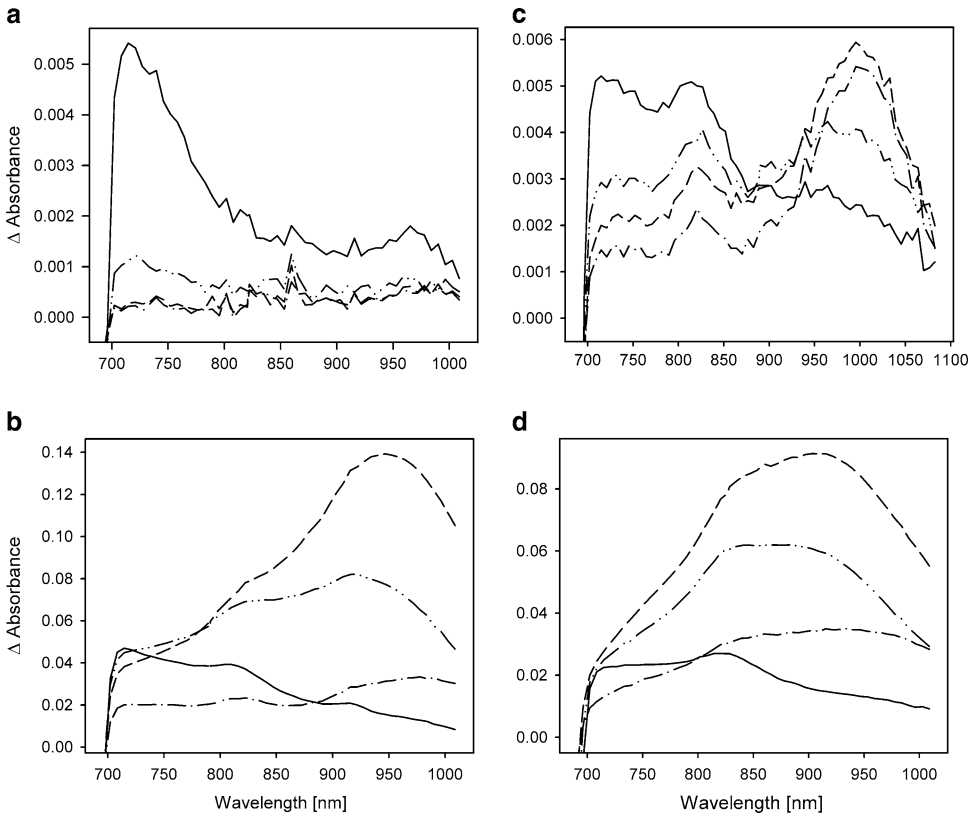

Fig. 1 Light-induced NIR absorbance difference spectra of PSII core and 5ChlRC preparations at different times during the illumination in the presence of artificial electron acceptors. (**a**) 5ChlRC + FeCy, (**b**) 5ChlRC + FeCy + SiMo, (**c**) PSII core + FeCy, (**d**) PSII core + FeCy + SiMo. Only positive difference absorption is showed for visualization purposes. For experimental conditions, see "Materials and methods". Times of spectra capture after turning actinic light on are indicated by line style as follows: dashed dotted—0.1 s; dashed—1 s; dashed double-dotted—10 s; solid line—60 s

To eliminate the possibility of direct oxidation of β-carotenes by SiMo in illuminated PSII and 5ChlRC samples, we have performed a series of measurements with red actinic light (>640 nm) which is not absorbed by β-carotene. Virtually identical results were observed which proves that β-carotene is oxidized either directly or indirectly by interaction with oxidized primary donor $P680^+$ (data not shown).

The identity of oxidized β-carotene should be recognized from its blue absorption, as the two β-carotenes of the PSII RC were suggested to differ in their absorption maxima (Tomo et al. 1997). Figure 2 shows the light-induced absorbance difference spectra in the carotenoid region of PSII core and 5ChlRC in the presence of SiMo (FeCy was omitted in these experiments because of its strong absorption in this region) as the electron acceptor. Ten subsequent measurements were done on one fresh sample. The illumination has resulted in irreversible bleaching of β-Car absorption different for 5ChlRC and PSII core complexes. In 5ChlRC maximum bleaching is positioned at 485 nm with another peak at 456 and a shoulder at 507 nm. Measurements during subsequent illuminations yield spectra with the same peak positions but some difference in their amplitudes. The main feature can be observed between the first and the second measurement at 507 nm absorption. During the first experiment, a well-pronounced shoulder at 507 nm can be seen, which disappears in the next measurements. During the 10 subsequent illuminations the sample lost 30% of its initial 484 nm absorption.

In core complexes, bleached spectra have two peaks of similar height, centred at 494 and 461 nm. During subsequent illuminations, the 494 nm peak is slightly blue-shifted to approximately 489 nm. No difference between subsequent measurements as in 5ChlRC was observed. Sixty percent of the 492-nm absorption of fresh sample was lost during these 10 illuminations.

Kinetic traces of peaks from the NIR spectra in Fig. 1a, b, c, d are shown in the respective panels of Fig. 3. For 5ChlRC with FeCy, only the P680 cation kinetic is detectable (Fig. 1a), showing its linear increase with the length of illumination (Fig. 3a). The PSII core complexes with FeCy show more complex behaviour. The β-Car cation (shown as 1,002 nm trace) peaks at $\sim$0.2 s and starts to recede at $\sim$0.4 s. The 820-nm peak of Chl_ZD1 accumulates slightly faster than $P680^+$ during onset of actinic illumination. Both chlorophyll cations have two-phase kinetic with fast increase at the beginning of the illumination and a second increase after β-Car^+ starts to decay (Fig. 3c).

NIR data from 5ChlRC and PSII core complexes measured with SiMo and FeCy in the range of 800–1,000 nm were globally fitted with sums of three gaussians yielding components with reproductively distinct positions. Those

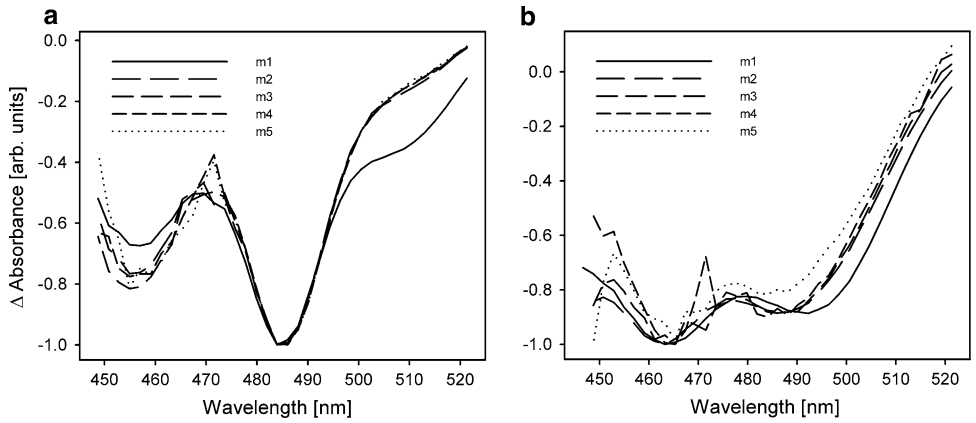

Fig. 2 Series of subsequent illumination experiments on single sample. Difference absorption spectra of 5ChlRC (**a**) and PSII core complexes (**b**) after 60 s of actinic illumination in the presence of SiMo. Spectra were normalized at maximum bleaching. Lines m1–m5 correspond to individual subsequent measurements; m1 is the first measurement with fresh sample; m5 is the last measurement after four previous experiments performed on the same sample

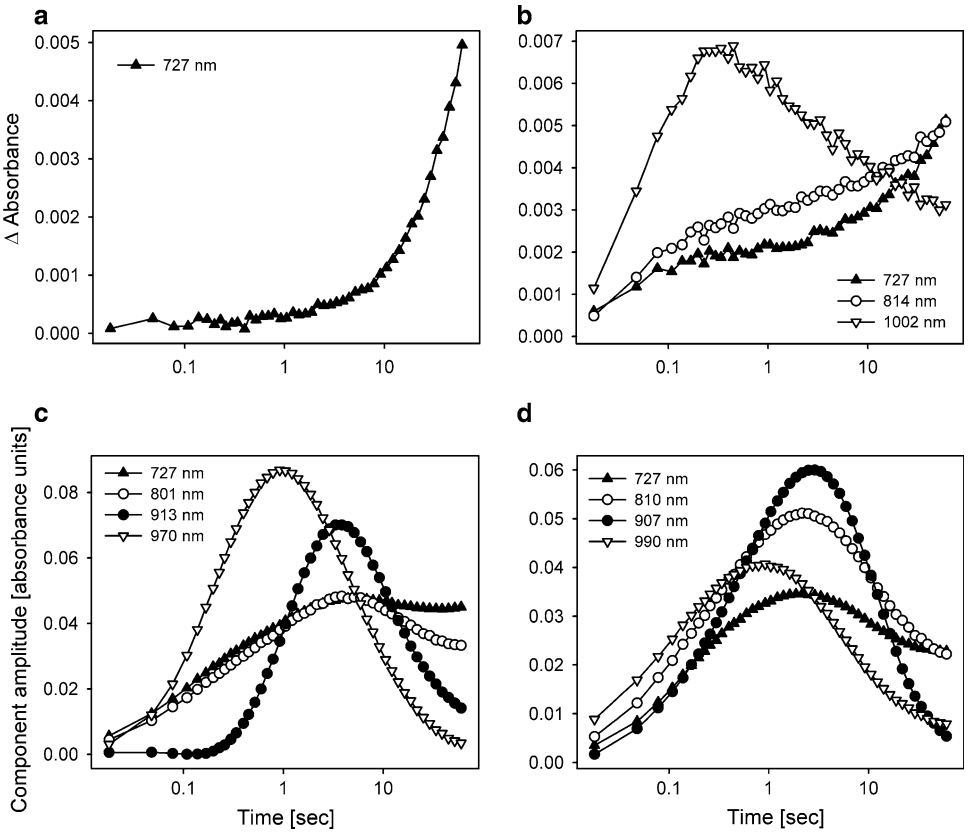

Fig. 3 Absorbance and amplitudes of gaussians fitted globally to the data from Fig. 1 plotted against time of spectra capture. (**a**) 5ChlRC + FeCy, (**b**) 5ChlRC + FeCy + SiMo, (**c**) PSII core + FeCy, (**d**) PSII core + FeCy + SiMo. The time is in a logarithmic scale. Kinetics at 727 nm and all data in panels **a** and **c** are actual measured data; panels **b** and **d** also contain kinetics of fitted gaussian bands whose maxima are indicated

were 800–820 nm, which we ascribe to peripheral chlorophyll cation(s), 900–930 nm, which we presume to be an unknown carotenoid cation(s), and 970–1,020 nm, which we assume to be β-carotene cation(s) (see discussion for details of peak assignment). Kinetics of amplitudes of the three fitted components are shown in Fig. 3b, d.

Figure 3b shows the kinetics of amplitudes of three fitted components at 801, 913 and 970 nm and the peak of P680 cation at 727 nm of 5ChlRC in presence of FeCy and SiMo. There is significant difference in kinetic properties of the fitted maxima. The 970-nm peak of β-carotene cation accumulates fast and after about 1 s of illumination it starts to recede. It seems that it is substituted by another absorbing cation with maximum around 915 nm which does not appear until there is a significant amount of β-Car$^+$. Peripheral chlorophyll cation (Chl$_Z^+$)

spectrum is accumulated slowly and is less dramatically affected by photodestruction later into the illumination. It is worth to note that during subsequent illuminations only changes to the Chl_Z^+ and $P680^+$ peaks are partially reversible and during the 10th subsequent 60 s illumination the Chl_Z^+ band still accumulates to about 40% of maximum development during the first illumination. Similar, though not so pronounced, behaviour was observed on the PSII core complexes (Fig. 3d). Relative proportions of maximum amplitudes of fitted components differ among different datasets even if those were measured using the same protein isolation. However, the times of peaking do not change significantly among experiments.

In order to identify the nature of the 915-nm absorbing cation, we have run HPLC analyses of both illuminated and intact samples. Figure 4 shows comparison of the pigment composition between 5ChlRC sample before and after illumination in the presence of SiMo. The chromatogram of the pigment extraction from the intact sample consists of the chlorophyll *a* eluting at ~22 min, pheophytin *a* (at ~37 min) and *β*-carotene at 44 min. Traces of more polar xanthophylls are also detectable (at ~8 and ~12 min). The most visible change in the illuminated sample is a significant decrease of *β*-carotene amount (44 min). Further, several new pigments can be detected at 24, 34 and 35 min. All of these pigments have carotenoid-like absorption spectrum and are more polar than *β*-carotene. The amount of these new carotenoid species and the decrease in *β*-carotene content are positively correlated with the length of the actinic light treatment of the sample. Identical analysis run on the PSII core sample showed only the decrease of *β*-carotene content. No new pigments were observed (data not shown).

Discussion

Figure 1 shows light-induced absorption difference spectra of 5ChlRC and PSII core complexes in presence of FeCy or a mixture of FeCy and SiMo as electron acceptors. Difference spectra of 5ChlRC with FeCy in Fig. 1a show only the contribution of $P680^+$ which was also identified by its characteristic 435 and 682 nm bleaching (not shown, Vacha et al. 2005; Bina et al. 2006). Comparison of the 60 s spectrum of the FeCy-treated 5ChlRC (Fig. 1a) with the spectrum of FeCy- and SiMo-treated 5ChlRC (Fig. 1b) shows two additional peaks with maxima at ~810 and ~915 nm in the later sample. Based on the work of Tracewell et al. (2001), we have assigned the ~810-nm shoulder to the oxidized peripheral chlorophyll molecule Chl_ZD1. However, this assignment is not without doubts. The 5ChlRC lacks one of the peripheral chlorophyll molecules as opposed to "common" six-chlorophyll PSII RC; the position of the remaining peripheral chlorophyll is still not clear. Based on PSII protein structure, we suppose that since Chl_ZD2 is partially shielded by PsbI and Cyt b_{559} proteins it is likely that Chl_ZD1 is presumably more easily extracted by metal affinity chromatography. However, recently the presence of Chl_ZD1 in 5ChlRC was proposed based on the chlorophyll to *β*-carotene triplet transfer (Arellano et al. 2007). As no ~850 nm peak which should according to Tracewell et al. (2001) belong to the Chl_ZD2 was observed in any of our experiments, Chl_ZD2 appears to be missing in the 5ChlRC isolation. On the other hand, recent structural data (Ishikita et al. 2007) indicate that Chl_ZD2 is the pigment which is preferentially oxidized by $P680^+$, since Chl_ZD1 and its nearby *β*-carotene are too far away from both $P680^+$ and other pigments to form an efficient cation sink.

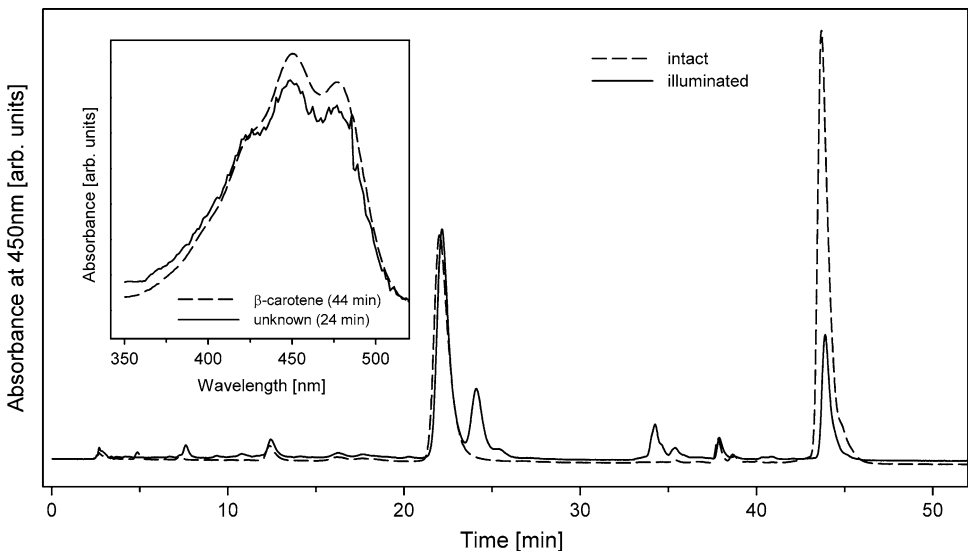

Fig. 4 Comparison of HPLC chromatograms of PSII 5ChlRC before and after illumination by actinic light in the presence of SiMo. Sample was illuminated five times for 60 s with 900 s dark relaxation between subsequent illuminations. Chromatograms were normalized to the amplitude of the peak at 22 min (Chl *a*). Inset: absorption spectra of *β*-carotene (eluting at 44 min) and unknown carotenoid eluting right after the Chl *a* at 24 min

Figure 1c shows different behaviour of PSII core complexes with FeCy when compared with 5ChlRC. Besides $P680^+$ absorption there are also distinct ~820 and 999 nm peaks which are at the exact locations of Chl_ZD1^+ and β-Car^+ species as described by Tracewell and Brudvig (2003), Hanley et al. (1999) and Faller et al. (2001). During subsequent illuminations the 999-nm peak is still accumulated (with increasingly smaller yield). This is probably due to low $P680^+$ yield as compared to experiments, where also SiMo was added. Because the percentage of RCs oxidized during one illumination is lower, the β-carotene depletion rate is also lower.

Figure 1b and d demonstrates that using SiMo as an electron acceptor induces strikingly different behaviour than using FeCy. Both 5ChlRC and core complexes show massive positive differential absorption above 900 or 850 nm regions, respectively. We were not able to distinguish absorption peaks in other way than by fitting gaussian functions on the spectra. Global fitting with shared gaussian positions and widths used all information from single experiment to assign better peak positions and provided higher peak properties stability than by fitting single spectra one after another. Even so the dispersion of fitted peak positions among different datasets was around ±15 nm. Fits of the data from both 5ChlRC and PSII core complexes yield broad peak at 970–1,000 nm which, according to, e.g. Hanley et al. (1999), Telfer et al. (2003) and Tracewell and Brudvig (2003) we assign to the β-Car cation absorption. The second fitted far red peak at ~915 nm has width similar to the β-carotene one and is located in the region of carotenoid cation absorption, and we presume that it does belong to some unidentified carotenoid cation. The ~915-nm peak cannot be a vibration band of ~1,000 nm cation radical because of its different kinetic properties.

The β-Car bleaching in 5ChlRC (Fig. 2a) appears to be identical with 'in situ' spectrum of β-Car measured in pea PSII RC by Telfer et al. (1991). Although the 507-nm shoulder in the first illumination experiment suggests that the molecule which is bleached is the CarD2; it may be that CarD1 also possesses a small 507-nm shoulder or that the 5ChlRC sample is heterogeneous, and a small percentage of isolated centres contains either both Cars or only CarD2.

The PSII core bleaching (Fig. 2b) suggests a shorter wavelength β-Car is affected. The amount of total bleaching is approximately two times higher after 10 illuminations in the case of PSII cores when compared with 5ChlRC, which suggests that there is a massive loss of inner antenna β-carotenes. The approximately two times higher loss of β-Car absorption in PSII core complexes as compared to 5ChlRCs could be explained by the loss of both RC β-Cars. However, we consider this explanation unlikely because of structural differences between these two molecules and, especially, because of different pigment composition of illuminated 5ChlRC and core samples (see below), which indicates different photochemistry of these isolations during illumination in the presence of electron acceptors.

As it is clear from Fig. 3b, the 913-nm component is not present in the spectra until significant β-Car^+ absorption is accumulated. Because there is only one β-Car in 5ChlRC, we presume that the ~915-nm species is a cation of unspecified carotenoid-like product of the original β-Car molecule which was modified by $P680^+$ oxidation. The possibility that the ~915-nm peak belongs to the second β-Car present in the RC is implausible since firstly, there is only about 1.1 β-Car per 5ChlRC as judged from HPLC pigment analyses (Vacha et al. 1995); secondly, the β-Car should be oxidized relatively fast because of its proximity to $P680^+$, e.g. Kitajima and Noguchi (2006) report full oxidation within 2 s at 80 K, and at room temperature the speed can be expected to increase significantly; thirdly, we are not aware of reports of wild type protein-embedded β-Car cation absorbing way below ~970 nm. The explanation of the ~915-nm peak as an unbound β-Car^+ seems also unlikely, because the position of the cation band of the unbound β-Car is usually in the region of 989-1,000 nm (Jeevarajan et al. 1996; Galinato et al. 2007), and it is difficult to imagine its generation by red actinic light (>640 nm) used for the 5ChlRC illumination. The ~915-nm peak could theoretically be the absorption of β-Car dication, but it was reported before by Jeevarajan et al. (1996) by about 100 nm to the shorter wavelengths at 817 nm.

On PSII core complexes (Fig. 3d) the 907- and 990-nm peaks arise almost simultaneously though their kinetics are clearly different. We suppose the peak assignment identical to 5ChlRC (see above). The main difference between PSII core and 5ChlRC is however seen in HPLC pigment analyses (Fig. 4). Illuminated 5ChlRC yielded three new carotenoid species, but core complexes did not yield any new carotenoids (PSII core data not shown). It was calculated before that the PSII inner antenna may serve as an efficient cation sink and thus protect the reaction centre from oxidative damage (Ishikita et al. 2007). In our experiments (Fig. 1d), the β-carotenes of PSII core complexes were depleted by actinic illumination which means that PSII pigments are still damaged by the cations unquenched by water-originating electrons. However, based on our HPLC data, it seems that the photodegradation of PSII core β-carotenes is a different mechanism than in 5ChlRC.

In light of this conclusion it may be possible that the 907-nm radical is located in the inner antenna and is not identical to the ~915-nm radical of 5ChlRC. The photoaccumulation of 907 nm radical of PSII core complexes

starts earlier than photoaccumulation of the ~915-nm radical in 5ChlRC which may be explained by efficient transport of cations from PSII RC to the inner antenna.

In our conditions the peripheral chlorophyll was photooxidized even after β-Cars were depleted which seems to be in-line with the data of Kitajima and Noguchi (2006) who found that at 80 K β-Car is not necessarily a member of an electron transfer chain between $P680^+$ and Chl_Z. On the other hand, Kitajima and Noguchi also observed increased significance of β-Car at higher temperatures (210 K) and lowered Chl_Z^+ yield after β-Car depletion. Although our Chl_Z^+ yield also declined with each illumination experiment, we believe it was mostly caused by unspecified photodamage to the sample and not by the β-Car depletion. We have not observed changes in $P680^+$ versus Chl_Z^+ ratios during subsequent illuminations, as one would expect if ChlZ oxidation was dependent on β-Car content. Our kinetic NIR data (Fig. 3) do not suggest any functional connection between Car cation reduction and peripheral chlorophyll oxidation or vice versa, although this is probably due to low time resolution and usage of continuous actinic light in our measurements. It is interesting that we were able to see β-Car cations at room temperature as all low temperature studies indicate diminishing Car^+ yields with increasing temperature, especially above 200 K (e.g. Schenck et al. 1982; Hanley et al. 1999; Tracewell et al. 2001).

The novel carotenoid product of the illuminated 5ChlRC has significantly shorter retention time than β-Car (24 vs. 44 min, Fig. 4) indicating large increase of polarity. Absorption spectrum of the 24-min pigment (Fig. 4, inset) resembles closely the absorption spectrum of β-Car which indicates that the conjugate bond chain is probably intact. Also, the resolution of the carotene vibronic bands should increase with shortening of the conjugated double bond chain (Galinato et al. 2007) which does not seem to be our case. Fiedor et al. (2001) have conducted detailed photodegradation analysis of solutions of bacteriochlorophyll and β-carotene and pigment VII from their analyses that bears some resemblance to our 24 min species (the other pigments in their analyses have absorption significantly different from β-Car and therefore cannot be directly linked to our data). It has very similar absorption maxima to β-Car and its retention time is ~66% of the β-Car retention time (our 24 min species has ~55% retention time versus β-Car). Moreover, the mass spectrometry of pigment VII indicates the mass of β-Car plus one oxygen atom, and a chemical reactivity test showed possible epoxide or vicinal diol group. Therefore, the most probable explanation of our HPLC data is that the β-Car of PSII RC has been modified by creation of some polar, perhaps oxygen-containing, group outside of the conjugated double bond chain due to a photooxidation.

Conclusion

We have shown that β-carotene and peripheral chlorophyll cations are produced in PSII RC and PSII core isolations in the presence of electron acceptors at room temperature. We have confirmed that peripheral chlorophyll is photooxidized even after β-carotene depletion in both 5ChlRC and PSII core complexes. We have observed that novel carotenoids are produced by actinic illumination in 5ChlRC but not in PSII core complexes. The hypothesis that inner antenna pigments form cation sink connected to the PSII RC which protects the reaction centre pigments from photodamage has therefore been experimentally confirmed.

Acknowledgements The authors would like to thank I. Hunalová and F. Matoušek for preparation of the samples. This work was supported by institutional support AV0Z50510513, MSM6007665808 and grants GACR 206/06/0322 and GAAV A608170604.

References

Arellano JB, Perez SG, Melo TB, Vacha F, Naqvi KR (2007) A reaction center of photosystem II with no peripheral pigments in D2 allows secondary electron transfer in D1. Biochemistry 46:15027–15032

Bina D, Litvin R, Vacha F, Siffel P (2006) New multichannel kinetic spectrophotometer-fluorimeter with pulsed measuring beam for photosynthesis research. Photosynth Res 88:351–356

Durrant JR, Klug DR, Kwa SL, van Grondelle R, Porter G, Dekker JP (1995) A multimer model for P680, the primary electron donor of photosystem II. Proc Natl Acad Sci USA 92:4798–4802

Faller P, Pascal A, Rutherford AW (2001) β-carotene redox reactions in photosystem II: electron transfer pathway. Biochemistry 40:6431–6440

Fiedor J, Fiedor L, Winkler J, Scherz A, Scheer H (2001) Photodynamics of the bacteriochlorophyll–carotenoid system. 1. Bacteriochlorophyll-photosensitized oxygenation of β-carotene in acetone. Photochem Photobiol 74:64–71

Frank HA, Brudvig GW (2004) Redox functions of carotenoids in photosynthesis. Biochemistry 43:8607–8615

Galinato MGI, Niedzwiedzki D, Deal C, Birge RR, Frank HA (2007) Cation radicals of xanthophylls. Photosynth Res 94:67–78

Hanley J, Deligiannakis Y, Pascal A, Faller P, Rutherford AW (1999) Carotenoid oxidation in photosystem II. Biochemistry 38:8189–8195

Hillmann B, Schlodder E (1995) Electron transfer reactions in photosystem II core complexes from Synechocossus at low temperature—diference spectrum of $P680^+Q_A^-$/P680QA at 77 K. Biochim Biophys Acta 1231:76–88

Ishikita H, Loll B, Besiadka J, Kern J, Irrgang K-D, Zouni A, Saenger W, Knapp E-W (2007) Function of two β-carotenes near the D1 and D2 proteins in photosystem II dimers. Biochim Biophys Acta 1767:79–87

Jeevarajan JA, Wei CC, Jeevarajan AS, Kispert LD (1996) Optical absorption spectra of dications of carotenoids. J Phys Chem 100:5637–5641

Kitajima Y, Noguchi T (2006) Photooxidation pathway of chlorophyll Z in photosystem II as studied by FTIR. Biochemistry 45:1938–1945

Kuta Smatanova I, Gavira JA, Rezacova P, Vacha F, Garcia-Ruiz JM (2006) New techniques for membrane protein crystallization tested on photosystem II core complex of *Pisum sativum*. Photosynth Res 90:255–259

Loll B, Kern J, Saenger W, Zouni A, Biesiadka J (2005) Towards complete cofactor arrangement in the 3.0 Å resolution structure of photosystem II. Nature 438:1040–1044

Mathis P, Setif P (1981) Near-infrared absorption-spectra of the chlorophyll-a cations and triplet-state in-vitro and in-vivo. Isr J Chem 21:316–320

Raszewski G, Diner BA, Schlodder E, Renger T (2008) Spectroscopic properties of reaction center pigments in photosystem II core complexes: revision of the multimer model. Biophys J 95:105–119

Schenck CC, Diner B, Mathis P, Satoh K (1982) Flash-induced carotenoid radical cation formation in photosystem II. Biochim Biophys Acta 680:216–227

Stewart DH, Cua A, Chisholm DA, Diner BA, Bocian DF, Brudvig GW (1998) Identification of histidine 118 in the D1 polypeptide of photosystem II as the axial ligand to chlorophyll Z. Biochemistry 37:10040–10046

Telfer A, De Las Rivas J, Barber J (1991) β-carotene within the isolated photosystem II reaction centre: photooxidation and irreversible bleaching of this chromophore by oxidized P680. Biochim Biophys Acta 1060:106–114

Telfer A, Frolov D, Barber J, Robert B, Pascal A (2003) Oxidation of the two β-carotene molecules in the photosystem II reaction center. Biochemistry 42:1008–1015

Tomo T, Mimuro M, Iwaki M, Kobayashi M, Shigeru I, Satoh K (1997) Topology of pigments in the isolated photosystem II reaction center studied by selective extraction. Biochim Biophys Acta 1321:21–30

Tracewell CA, Brudvig GW (2003) Two redox-active β-carotene molecules in photosystem II. Biochemistry 42:9127–9136

Tracewell CA, Cua A, Stewart DH, Bocian DF, Brudvig GW (2001) Characterization of carotenoid and chlorophyll photooxidation in photosystem II. Biochemistry 40:193–203

Vacha F, Joseph DM, Durrant JR, Telfer A, Klug DR, Porter G, Barber J (1995) Photochemistry and spectroscopy of a five-chlorophyll reaction center of photosystem II isolated by using a Cu affinity column. Proc Natl Acad Sci USA 92:2929–2933

Vacha F, Durchan M, Siffel P (2002) Excitonic interactions in the reaction centre of photosystem II studied by using circular dichroism. Biochim Biophys Acta 1554:147–152

Vacha F, Psencik J, Kuty M, Durchan M, Siffel P (2005) Evidence for localisation of accumulated chlorophyll cation on the D1-accessory chlorophyll in the reaction centre of photosystem II. Photosynth Res 84:297–302

Wang J, Gosztola D, Ruffle SV, Hemann C, Seibert M, Wasielewski MR, Hille R, Gustafson TL, Sayre RT (2002) Functional asymmetry of photosystem II D1 and D2 peripheral chlorophyll mutants of *Chlamydomonas reinhardtii*. Proc Natl Acad Sci USA 99:4091–4096